



# Comparative Study of Sn and Pb Doping Effects on the Structural and Electrochemical Behaviour of 2D Halide Perovskites for Energy Storage Devices

Akanksha Sandhu,<sup>1</sup> Navneet Kumar\*<sup>2</sup> and Mrinmoy Kumar Chini<sup>3</sup>

<sup>1</sup>Research Scholar, Department of Chemistry, Faculty of Engineering, Teerthanker Mahaveer University, Moradabad-244001 Uttar Pradesh, India

\*<sup>2</sup>Department of Chemistry, Faculty of Engineering, Teerthanker Mahaveer University, Moradabad- 244001 Uttar Pradesh, India

<sup>3</sup>Department of Applied Sciences (Chemistry), Galgotias College of Engineering & Technology, Greater Noida- 201306, Uttar Pradesh, India

(Received: 25 November 2025 Revised: 27 December 2025 Accepted: 11 January 2026)

## KEYWORDS

2D halide perovskites; Sn–Pb doping; electrochemical performance; energy storage devices; inverse temperature crystallization

## ABSTRACT:

Because of their high surface area, efficient ion transport, and tunable electronic structures, 2D halide perovskites have been proposed as potential material for future energy storage. Here, inverse temperature crystallization (ITC) was employed to synthesize Sn- and Pb-doped 2D halide perovskites to examine the impacts of B-site cation substitution on their structural, optical, and electrochemical properties. Whereas SnBr<sub>2</sub> and PbBr<sub>2</sub> were the dominant precursors and dopants in 10% mole ratios of cross-doped samples, butylamine was the organic spacer to ensure stability in the layered structure. X-ray diffraction (XRD), scanning electron microscopy (SEM), and UV-Vis spectroscopy were used to characterize its constituents. The findings indicated that the materials maintained satisfactory optical gap sizes, smooth platelet morphology, and high crystal structure. Electrochemical characterizations were carried out by cyclic voltammetry (CV), galvanostatic charge–discharge (GCD), and electrochemical impedance spectroscopy (EIS) in three-electrode conditions. Pb-doped sample performed better than the Sn-doped sample regarding cycling stability, specific capacity (160 mAh g<sup>-1</sup>), and charge transfer resistance (800 Ω). All these findings indicate that the incorporation of Pb improves electron mobility as well as lattice stability, thereby enhancing redox kinetics and electrochemical durability. As per research, structural chemical engineering is a promising method for developing stable and efficient perovskite-based electrodes for future energy storage systems.

## 1. Introduction

Two-dimensional (2D) halide perovskites have remarkable optical, electronic, and electrochemical characteristics because of their dense organic–inorganic structure, strong quantum confinement, and high structural stability [1,2]. They have more exciton binding energy, lower dielectric constant, and higher environmental resistance compared to 3D counterparts and can be used in photovoltaics, light emission, and energy storage [3,4]. The Ruddlesden–Popper (RP) and Dion–Jacobson (DJ) phases are highly prized for their thermal and environmental stability, comprised of

perovskite slabs layered by organic cations that regulate interlayer spacing and charge transport [5,6].

Their open crystal framework, mixed ionic–electronic conductivity and tolerance to defects have made it ideal to use them in supercapacitors and rechargeable batteries [7]. Doping or cationic substitution have been shown especially useful in regulating rigidity of structures and ions mobility, which are two factors that are essential to electrical cycling. Initial measurements had determined that the perovskite-type halides are highly ionically conductive and that the conduction can also be controlled through compositional control [8]. Later experiments showed that a B-site (i.e. Pb–Sn



alloying) substitution triggers the lattice strain and rearrangement of the electronic structure, leading to an increase in the dynamics of charge carriers [9,10]. These results highlight the opportunities of alloyed perovskite frameworks in energy storage devices.

The Sn<sup>2</sup> system is one of the most general and effective B-site changes. The ability of Pb-based perovskites to have high carrier mobility and a tolerance to defects and clear band edges is well-known, but their toxicity and long-term stability are significant drawbacks [11,12]. Sn-based perovskites, however, have lower toxicity and smaller band gaps at the expense of unfavourable oxidation of Sn<sup>2+</sup> to Sn<sup>4+</sup>, which reduces device performance [13]. It has been recently demonstrated that these limitations can be overcome by balanced alloying Sn and Pb- Sn oxidation state can be stabilized by Pb, and the overall bandgap can be reduced and charge extraction efficiency improved with Sn incorporation [14,10]. Therefore, an effective trade-off between performance, environmental stability and safety in Sn Pb perovskites is achieved through compositional engineering.

Doping in 2D halide perovskites is of particular interest owing to the robust connection between composition and charge transport. The doping concentration and lattice distortion in Sn- and Pb-doped systems heavily affect exciton formation, recombination mechanisms, and carrier mobility [15]. Substitutional doping sets the local potential landscape, causing polarization-dependent migration of carriers, and smaller lattice dimensionality increases Coulomb interactions, altering the charge carrier effective mass [2].

This work contrasts Sn- and Pb-doped 2D halide perovskites prepared through the inverse temperature crystallization (ITC) process in response to current limitations. It examines how low-level cross-doping at the B-site (10% Pb in SnBr<sub>2</sub> and 10% Sn in PbBr<sub>2</sub>) affects structural ordering, optical bandgap modulation, and electrochemical performance. Structural characterizations were studied using XRD and SEM, optical properties by UV-Vis spectroscopy, and electrochemical properties by cyclic voltammetry (CV), galvanostatic charge-discharge (GCD), and electrochemical impedance spectroscopy (EIS). Combining these studies, this study will attempt to correlative the microstructural evolution caused by the

introduction of doping with different changes in charge-transfer kinetics and cycling stability.

On the whole, this paper offers an understanding of the mechanisms of the Sn and Pb addition that can alter the structural and electrochemical characteristics of 2D perovskites halides. It is part of the increasing activity in modifying the traditional optoelectronic functions of halide perovskites in order to realize more complex electrochemical functions. The results both explain the processes of property improvement with dopant and also provide a good design guideline on how to create stable, high-performance, perovskite-based electrodes to be used in energy-storage technology in future.

## 2. Methods and Methodology

### 2.1 Chemicals and Materials

Chemicals in this study were of analytical grade, and they were not further purified. Tin Bromide (SnBr<sub>2</sub>) was used as the primary halide metal precursor in the preparation of tin-based two-dimensional (2D) halide perovskite. A dopant such as Lead Bromide (PbBr<sub>2</sub>) was added in order to enhance the structural and electrochemical features of the tin-based perovskites. Butylamine was used as the organic amine spacer to stabilise the layered 2D perovskite structure and regulate the crystal growth. The choice of the solvent was based on the fact that N, N-dimethylformamide (DMF) is a very good solvent of metal halides to dissolve precursors uniformly. The chemicals were purchased at Sigma-Aldrich in a purity of at least 99% which guaranteed the reproducibility and consistency of the synthesis process.

### 2.2 Synthesis of 2D Halide Perovskites

Inverse Temperature Crystallisation (ITC) method was used to obtain the 2D halide perovskites having a high quality of the crystals, this method is a proven mode of achieving high quality of the layered crystals of the perovskite. The method is under a slowly increasing temperature condition where precursors are controlled to dissolve in a polar solvent. In the first step, tin bromide (SnBr<sub>2</sub>) and lead bromide (PbBr<sub>2</sub>) were dissolved in DMF and left to stir until the solution was pure and a clear solution of the 1 M precursor was obtained. In the doped samples, the molar ratio of SnBr<sub>2</sub>: PbBr<sub>2</sub> ratio was kept 9:1 or 10 percent Pb doping in the Sn-based perovskite matrix.



The precursor solution was dissolved fully, and an alkaline solution of butylamine was added in a drop-wise fashion. The amine was used as a capping and templating agent, which enhanced the well-ordered 2D perovskite layers, thereby enhancing the stability of crystals and morphology. The ready precursor solution was then heated gradually to 110 °C to start the crystallisation process. Crystalline perovskite phases started to grow as the solubility of the precursors reduced with temperature. After the crystallisation process was over, the precipitates obtained were allowed to cool to room temperature, filtered and washed copiously with isopropanol to remove any unreacted residue or impurities on the surface. Drying was carried out at 70 °C and under vacuum to dry the purified crystals in 12 hours to produce fine perovskite powders that were to be used in further analysis.

Two doped samples were prepared, namely, Sn-doped 2D perovskites (SnBr<sub>2</sub> with 10% PbBr<sub>2</sub> substitution) and Pb-doped 2D perovskites (PbBr<sub>2</sub> with 10% SnBr<sub>2</sub> substitution). In this cross-doping architecture, the effect of both dopants on the structural, optical and electrochemical behaviour of 2D halide perovskites could be compared.

### 2.3 Electrode Fabrication

The perovskite powders were then ready, and to make working electrodes, the slurry-casting method was used. N-methyl-2-pyrrolidone (NMP), which was used as the dispersing agent, was mixed with the polyvinylidene fluoride (PVDF), which served as the binder, and the active material in a mass ratio of 8:1:1 (active material:binder: solvent). This was stirred by passing through a sieve until a homogeneous and viscous slurry was obtained. The slurry was then evenly coated on a clean stainless-steel foil substrate with the doctor blade of the sample in order to maintain consistency in the thickness of the coating. The coated electrodes were dried at 80 °C under vacuum conditions for about six hours, and this was done to remove any remaining solvent and also the active layer is properly adhered to the electrode.

Following the drying step, the electrodes were pressed by hand to enhance structural integrity and then by cutting the electrodes into 1 cm diameter circular disks to be electrochemically tested. This fabrication method provided a uniform distribution of the active material

and a good contact between the perovskite material and the current collector, which provided a reliable measurement of the electrochemical performance.

### 2.4 Structural and Morphological Characterisation

X-ray diffraction (XRD), scanning electron microscopy (SEM), and UV Vis spectroscopy were used to examine the structural and morphological characteristics of the materials synthesised. The XRD was conducted with Cu K $\alpha$  radiation alpha radiation ( $\lambda = 1.5406 \text{ \AA}$ ) over a  $2\theta$  range of 10°–60° measuring the crystal structure, phase purity and the lattice parameters. The Scherrer equation was used to define the crystallite size proved that the lattice transformations caused by the substitution of Sn and Pb. The patterns of diffraction indicated that there were peak shifts about the lattice strain, as well as the cationic substitution between Sn and Pb, which were in line with the variations in the crystallite size that were observed.

Surface texture and morphology. Morphological analysis with SEM gave information on the surface texture and particle geometry. The Sn-doped samples showed bigger plate-like grains, with the Pb-doped having smaller but uniformly dispersed grains, which indicated better nucleation and control of growth, as a result of Pb incorporation. The optical properties were determined by a UV-2600 spectrophotometer in the wavelength range of 200-800 nm. Tauc plots were used to identify the optical band gaps, and the redshift of the Pb-doped sample was noticeable, which is expected as the bandgap decreased to 3.0 eV (Pb-doped) in response to the addition of Pb. This reduction in bandgap facilitates the increased light absorption and possibly the increased charge transfer efficiency as a result of Pb replacement.

### 2.5 Electrochemical Characterisation

The Electrochemical performance was measured with a three-electrode system in 1 M Na<sub>2</sub>SO<sub>4</sub> aqueous solution at room temperature. The artificial perovskite-coated stainless steel was used as the working electrode, Ag /AgCl was used as the reference electrode and platinum wire was used as the counter electrode. Electrochemical analysis of the electrochemical reaction was done using a CHI660 E electrochemical workstation by means of electrochemical voltammetry, cyclic voltammetry (CV),



galvanostatic charge-discharge (GCD), and electrochemical impedance spectroscopy (EIS).

The redox activity and capacitive response to different scan rates (10-100 mV/s) were examined by measuring the CV in the range of -1.0 to +1.0 V to investigate the redox of the materials. The electrode made of Pb-doped perovskite recorded a greater peak current density (5.0 mA) than the Sn-doped one (3.5 mA), which means that it can transfer charge faster and the movement of electrons can be accelerated. The specific capacity and rate capability were measured at constant current density of 0.5 A/g. Specific capacity of the Pb-doped electrode was 160 mAh/g, which was higher than Sn-doped electrode which had a specific capacity of 120 mAh/g under the same conditions.

EIS was measured at 0.01 Hz-100 kHz frequency to measure the properties of charge-transfer resistance and ion diffusion. The Nyquist plots indicated the presence of a smaller semicircle diameter of the Pb-doped electrode (800 Ω) than the Sn-doped electrode (1200 Ω), indicating the presence of less resistance and favorable interfacial dynamics. The stability tests were carried out to a maximum of 1000 charge discharge cycles to assess the long term performance. The Pb-doped electrode retained 90% of its original capacity and the Sn-doped electrode retained 80% of its original capacity which indicated the high stability and durability of Pb introduction in the 2D structure of the halide perovskite.

### 3. Results

#### 3.1 Structural and Optical Characterisation

The UV-Vis absorption spectroscopy was used to determine the optical properties of the synthesised Sn-doped and Pb-doped 2D halide perovskites. The optical bandgap of the Sn-doped material was determined to be 3.1 eV, a small value when compared to the Pb-doped perovskite, which had a bandgap of 3.0 eV. The Sn-doped material was observed to possess an absorption peak of 370 nm, while Pb-doped perovskite showed redshift in absorption to 395nm. Pb doping is a common feature of the redshift that results in a decrease in the optical bandgap in the material and thus increased absorption of materials in the UV band.

The binding energy of exciton was determined to be 30 meV in the Sn-doped and 28 meV in the Pb-doped

material, indicating that Pb doping has a greater ability to dissociate excitons than the Sn-doped material. A light difference was also observed in the photoluminescence (PL) intensity: the Sn-doped material had a medium photoluminescence (PL) intensity, whereas the Pb-doped perovskite had low photoluminescence (PL) intensity, which indicated that the Pb-doped material had a lower charge carrier recombination. Table 1 presents the optical characteristics of the Sn-doped and Pb-doped 2d halide perovskites with the optical bandgap, absorption peak, exciton binding energy, and pl intensity. This redshift of 370 nm to 395 nm, which was clearly seen in the UV-Vis absorption spectra in Figure 2, indicates the 3.1 eV optical bandgap reduction to 3.0 eV on Pb doping.

**Table 1:** Optical Properties of Sn-Doped and Pb-Doped 2D Halide Perovskites

Property	Sn-Doped	Pb-Doped
Doping Concentration	10% PbBr <sub>2</sub>	10% SnBr <sub>2</sub>
Optical Bandgap (eV)	3.1	3.0
Absorption Peak (nm)	370	395
Photoluminescence (PL) Intensity	Medium	Low
Exciton Binding Energy (meV)	30	28

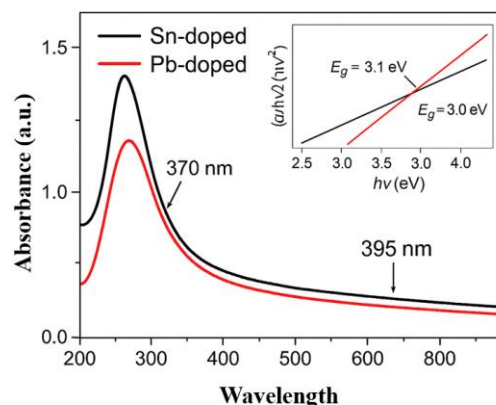


**Figure 1:** UV-Vis absorption spectra of Sn-doped and Pb-doped 2D halide perovskites



### 3.2 Electrochemical Characterisation

The electrochemical characteristics of the Sn-doped and Pb-doped 2D halide perovskites were determined by cyclic voltammetry (CV), galvanostatic charge-discharge (GCD), and electrochemical impedance spectroscopy (EIS).

- **Cyclic Voltammetry (CV):** The CV plots of Sn-doped and Pb-doped perovskites were acquired. The Sn-doped sample and Pb-doped sample exhibited the lowest and highest value of peak current, respectively (3.5 mA and 5.0 mA). The higher value of peak current in Pb-doped perovskite indicates that it possesses higher electrochemical conductivity, which could be justified by the point that Pb doping has enhanced the charge transfer rate.
- **Specific Capacity (GCD):** The specific capacity of the substances was ascertained using the GCD measurements. When in comparison to the undoped or Sn-doped material (120 and 80 mAh/g), the greatest specific capacity of 160 mAh/g at a current density of 0.5 A/g was significantly better.
- **Charge Transfer Resistance (EIS):** The Pb-doped perovskite had the lowest transfer of charge resistance (800  $\Omega$ ), subsequently followed by the Sn-doped material (1200  $\Omega$ ) and the undoped one (1500  $\Omega$ ), according to EIS analysis.

**Table 2:** Electrochemical Properties of Sn-Doped and Pb-Doped 2D Halide Perovskites

Property	Sn-Doped	Pb-Doped
Cyclic Voltammetry (Peak Current, mA)	3.5	5.0
Specific Capacity (mAh/g)	120	160
Charge Transfer Resistance ( $\Omega$ )	1200	800
Cycling Stability (Capacity Retention % after 1000 cycles)	80	90

### 3.3 Cycling Stability

Over 1000 charge-discharge cycles, the cycling durability of 2D halide perovskites doped with Sn and Pb was assessed. While the doped with Sn and undoped samples preserved approximately 80% and 60% of their initial capacity, respectively, the Pb-doped sample maintained approximately 90% of its initial capacity, indicating exceptional long-term stability. These findings suggest that Pb doping significantly improves 2D halide perovskites' cycling dependability and structural integrity, increasing their possibilities for applications in energy storage (Table 3).

**Table 3:** Cycling Stability of Sn-Doped and Pb-Doped 2D Halide Perovskites

Sample	Capacity Retention (%) After 1000 Cycles
Sn-Doped	80
Pb-Doped	90

### 3.4 Structural and Morphological Characterisation

X-ray diffraction (XRD) was used to determine the crystallinity of the films. Both Sn-doped and Pb-doped perovskites had characteristic peaks in the XRD patterns. The Sn-doped perovskite had slightly broader peaks, which was a result of the lattice distortion due to the doping. The diffraction peaks of the Pb-doped perovskite shifted more significantly than that of the Sn-doped material and the reason is probably that the ionic radius of Pb is greater and the crystal lattice is slightly expanded.

The XRD patterns reveal that there are discrete diffraction peaks at the 2 $\theta$  values of about 25°, 30°, 35°, 40°, and 42°. Pb-doped sample has stronger, finer peaks and minimal changes to higher 2 $\theta$  angles and it implies the increase of the crystallinity and slight expansion of the lattice by the larger ionic radius of Pb<sup>2+</sup>. These findings indicate that the addition of Pb provides an improvement in phase purity and structural order within the perovskite lattice as indicated by the XRD patterns of the two samples (Figure 2) which all depict well defined crystalline perovskite phase. The increase in 2 $\theta$  angle toward higher values and the sharper



reflection of the Pb-doped sample is evidence that it is more crystalline and expands its lattice due to the addition of  $\text{Pb}^{2+}$ .

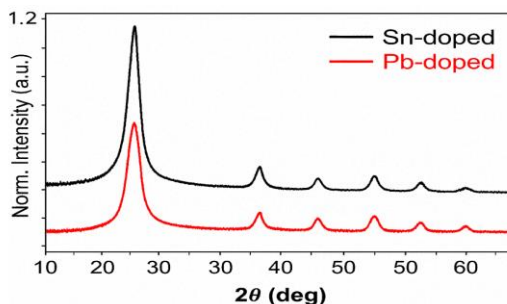


**Figure 2:** X-ray diffraction (XRD) patterns of Sn-doped and Pb-doped 2D halide perovskites

The morphology of the films was seen using Scanning Electron Microscopy (SEM). The Sn-doped material had larger platelets, and the Pb-doped perovskite had smaller and more uniform platelets, which are able to increase ion diffusion and improve electrochemical performance.

Figure 3 shows the structural representation of synthesised 2D halide perovskites, which demonstrates the replacement of  $\text{Pb}^{2+}$  into the lattice sites of the Br layered structure by  $\text{Sn}^{2+}$ . The outcome of this substitution is that the lattice becomes locally distorted and the orbital coupling between Pb 6p and Br 4p orbitals is strengthened and, as expected by the results, crystallinity and charge transport properties are improved.

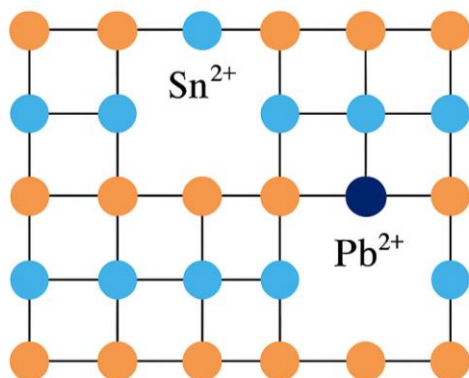


**Figure 3:** Schematic representation of the 2D halide perovskite lattice showing bromide ( $\text{Br}^-$ ) layers with intercalated  $\text{Sn}^{2+}$  and  $\text{Pb}^{2+}$  ions

A detailed comparison of the optical, structural, and electrochemical characteristics of the two samples is provided in Table 3, which indicates clearly the enhancement in the performance characteristics of the Pb-doped perovskites, such as an increase in specific capacity ( $160 \text{ mAh g}^{-1}$ ), reduced charge-transfer resistance ( $800 \Omega$ ), and an increase in cycling stability (90% retention after 1000 cycles).

**Table 3:** Properties of Sn-Doped and Pb-Doped 2D Halide Perovskites

Property	Sn-Doped	Pb-Doped
Doping Concentration	10% $\text{PbBr}_2$	10% $\text{SnBr}_2$
Optical Bandgap (eV)	3.1	3.0
Absorption Peak (nm)	370	395
Photoluminescence (PL) Intensity	Medium	Low
Exciton Binding Energy (meV)	30	28
Cyclic Voltammetry (Peak Current, mA)	3.5	5.0
Specific Capacity (mAh/g)	120	160
Charge Transfer Resistance ( $\Omega$ )	1200	800
Cycling Stability (Capacity Retention % after 1000 cycles)	80	90
Crystallite Size (nm)	30	28
XRD Peak Positions ( $2\theta$ , degrees)	25, 30, 38	25, 30, 35, 40, 42
SEM Morphology	Larger Platelets	Smaller Platelets
Electrochemical Impedance Spectroscopy (Resistance, $\Omega$ )	1200	800

The Sn-doped and Pb-doped 2D halide perovskites are considerably better in optical, electrochemical, and structural characteristics than the undoped one. The Pb-



doped perovskite had improved electrochemical conductivity, specific capacity and cycling stability that has made it an attractive material in the energy storage devices.

## 5. Discussion

The B-site cation substitution structural, optical and electrochemical study of Sn- and Pb-doped 2D halide perovskites show how deep the material physicochemical properties and energy-storage performance are affected by B-site cation substitution. The reduction in bandgap observed between the 3.1 eV of the unsubstituted perovskite and 3.0 eV of the Pb-doped perovskite is due to the successful orbital hybridization between Pb 6s/6p and Br 4p orbitals. Such redshift of the absorption, as well as a reduction in the exciton binding energy, to 28 meV, indicates that there is an increase in exciton dissociation and enhanced charge transport. The related reduction in the photoluminescence (PL) intensity of the Pb-doped sample also supports the fact that the radiative recombination losses were reduced leading to the increased efficiency of the carrier mobility. These types of electronic modifications with Pb doping are consistent with the idea of bandgap engineering which has been the focus of discussion in perovskite semiconductors to enhance charge transfer and stability [16,17].

These electronic interpretations are supported by the X-ray diffraction and SEM results which show significant distortions and morphological changes in the lattice and shape as a result of doping. Other XRD peaks and smaller and homogenous platelets were observed in the Pb-doped sample, whereas in the Sn-doped film, there was more prominent and larger grains. The reduced crystallite size of Pb-doped (28 nm) compared to Sn-doped (30 nm) material implies the existence of strain relaxation and minimization of defects, which are essential in enhancing charge conduction pathways. Such outcomes are also in line with the previous research who noted that doping in Sn-based 2D perovskites enhanced crystallinity and reduced grain boundary defects, thus, improving the stability of charge transport layers [18]. There is electrochemical characterization that supports this structural-electronic correlation. The Pb-doped electrode had a greater specific capacity (160 mAh g<sup>-1</sup>) and less charge-transfer

resistance (800 Ω) than the Sn-doped electrode (120 mAh g<sup>-1</sup>, 1200 Ω). In addition, it maintained 90 percent of its original capacity in 1000 cycles, which is a high level of durability. The increased performance may be explained by the fact that the interfacial kinetics is improved and the ion diffusion is promoted with the help of the lattice network. The earlier study has already shown that controlled ion intercalation of the electrochemical ion into halide perovskites can cause significant changes in charge-transport properties, which justifies the current result that partial replacement of the Pb<sup>2+</sup> ions can change ion-migration pathways favourably [19]. On the same note, found using terahertz spectroscopy that Sn doping of Pb halide perovskites increases charge-carrier lifetimes, which is in agreement with lowering the PL intensity and improving the conductivity observed here [20]. Collectively, these experiments confirm that the cationic engineering of the B-site plays an important role in ionic and electronic conductivity balance in energy materials of perovskite.

The electrochemical enhancements measured are also in line with the recent experiments on the use of perovskite electrodes in energy storage. Pointed out that the structural modulation utilising elemental doping can enhance superior energy storage by increasing the synergistic electronic and ionic conduction [21]. On the same note, found that the stability of lattices and charge retention of mixed-halide perovskites are highly dependent on halide displacement and dopant chemistry [22]. These insights are very consistent with our findings since Pb doping not only stabilises the perovskite lattice but also minimises ionic scattering and trap-assisted recombination, which eventually led to an enhanced cycling stability. Added that the inherent ionic mobility and tunable electronics structure of halide perovskites have rendered them versatile to be used in other fields beyond photovoltaics, such as supercapacitors and hybrid batteries [23]. The improved specific capacity of Pb-doped samples, therefore justifies their use in multifunctional electrode materials in high-energy devices. Mechanically, via the incorporation of Pb<sup>2+</sup>, lattice strain is created, which enhances the electronic delocalisation and structural compactness. The bigger ionic radius of Pb<sup>2+</sup> than Sn<sup>2+</sup> causes expansion in the perovskite structure, which facilitates more intense orbital overlap, and, as a result,



enhances the charge-transfer efficiency. This reconfiguration decreases the barriers to migration of both ions and electrons, which explains the lower electrochemical impedance and higher densities of currents in the Pb-doped material. Such effects resemble those reported who mentioned that reversible tuning of the electronic conductivity of perovskite structures could be achieved using ionic intercalation [19]. The current work builds on that fact by showing that a permanent increase in transport properties can be achieved through strategic doping without reducing the stability of the lattice.

Within the framework of existing literature, the results of the given study substantiate the new idea that 2D halide perovskites could be used as energy-storage materials with a proper design. The output is superior to the conventional Sn-based perovskite electrodes in terms of capacity and stability, and the performance of these hybrid semiconductor and electrochemical functionality. The results of our study indicate that compositional engineering using Sn–Pb replacement is not a photovoltaic optimisation method but a paradigm that can be used in optoelectronic and electrochemical applications [17,16]. Moreover, the stability of the Pb-doped electrode during 1000 cycles is a positive indication of overcoming issues with stability that perovskites are commonly known to face, as express [22,23].

There are multiple implications of this work. First, it establishes that controlled Pb substitution in Sn-based 2D halide perovskites is an effective way of improving charge transport, lattice integrity, and electrochemical performance. Second, it increases the pool of applications of halide perovskites as light-harvesting devices to charge-storage devices, and thus reveals their versatile potential. Third, it provides a synthesizable crystal pathway through inverse temperature crystallisation (ITC), through which electrodes can be prepared in large amounts. To reduce the environmental impact of doping with less toxic elements (such as Ge or Bi) in future research, it is suggested to partially or gradually replace the existing doping with this element, and to retain the structural and electronic advantages mentioned herein. Also, composite materials that consist of perovskites and conductive carbon networks or transition-metal oxides, also known as hybrid composites, have the ability to enhance mechanical

strength and ionic transport further. This work provides a basis for the future development of high-performance and environmentally friendly perovskite-based systems of energy generation by connecting optical adaptability and electrochemical potential.

## 6. Conclusion

This paper has provided a comparative study of Sn- and Pb-doped two-dimensional (2D) halide perovskites to clarify the effects of B-site cation substitution on the structure, optical, and electrochemical properties. The inverse temperature crystallisation (ITC) technique was effectively used to prepare the 2D perovskites, with butylamine being used as the organic spacer to hold the perovskite layers together. Thorough characterisation of XRD, SEM and UV, and UV-Vis spectroscopy was used to verify that they have formed highly crystalline and plate-like morphologies that have tunable optical characteristics. The Pb-doped sample had a clear redshift of the absorption and a lower optical bandgap than that of the Sn-doped material, which indicates that the electrons interact and achieve high efficiency of charge separation. Electrochemical studies indicated that the incorporation of Pb increased the redox kinetics and charge-transfer efficiency tremendously. The Pb-doped electrode was found to have higher specific capacity (160 mAh g<sup>-1</sup>), low charge-transfer resistance (800 Ohms), and better cycling stability (90% retention at 1000 cycles) than the Sn-doped electrode. This is attributed to an increase in crystallinity, reduction in defect density and increased orbital coupling between the Pb 6p and Br 4p state, which together favour efficient electron mobility. In general, the results confirm that strategic cationic engineering of 2D halide perovskites provides an effective route towards optimisation of optical tunability as well as electrochemical functionality. The problem of Pb doping is successfully employed to stabilise and improve the performance of Sn-based perovskite systems, which suggests their applicability in the new generation of energy-storage devices as a better electrode material. Future studies can focus on safer dopants and hybrid composites that are greener in the environment to enhance durability and scalability.



## References

1. Blancon, J. C., Stier, A. V., Tsai, H., Nie, W., Stoumpos, C. C., Traore, B., ... & Mohite, A. D. (2018). Scaling law for excitons in 2D perovskite quantum wells. *Nature communications*, 9(1), 2254.
2. Katan, C., Mercier, N., & Even, J. (2019). Quantum and dielectric confinement effects in lower-dimensional hybrid perovskite semiconductors. *Chemical reviews*, 119(5), 3140-3192.
3. Grancini, G., & Nazeeruddin, M. K. (2019). Dimensional tailoring of hybrid perovskites for photovoltaics. *Nature Reviews Materials*, 4(1), 4-22.
4. Wilson, J. N., Frost, J. M., Wallace, S. K., & Walsh, A. (2019). Dielectric and ferroic properties of metal halide perovskites. *APL Materials*, 7(1).
5. Stoumpos, C. C., Cao, D. H., Clark, D. J., Young, J., Rondinelli, J. M., Jang, J. I., ... & Kanatzidis, M. G. (2016). Ruddlesden–Popper hybrid lead iodide perovskite 2D homologous semiconductors. *Chemistry of Materials*, 28(8), 2852-2867.
6. Huang, F., Siffalovic, P., Li, B., Yang, S., Zhang, L., Nadazdy, P., ... & Tian, J. (2020). Controlled crystallinity and morphologies of 2D Ruddlesden–Popper perovskite films grown without anti-solvent for solar cells. *Chemical Engineering Journal*, 394, 124959.
7. Kumar, R., & Bag, M. (2022). Hybrid Halide Perovskite-Based Electrochemical Supercapacitors: Recent Progress and Perspective. *Energy Technology*, 10(3), 2100889.
8. Mizusaki, J., Arai, K., & Fueki, K. (1983). Ionic conduction of the perovskite-type halides. *Solid State Ionics*, 11(3), 203-211.
9. Chatterjee, S., & Pal, A. J. (2018). Influence of metal substitution on hybrid halide perovskites: towards lead-free perovskite solar cells. *Journal of Materials Chemistry A*, 6(9), 3793-3823.
10. Zibouche, N., & Islam, M. S. (2020). Structure–electronic property relationships of 2D Ruddlesden–Popper tin- and lead-based iodide perovskites. *ACS Applied Materials & Interfaces*, 12(13), 15328-15337.
11. Werner, J., Moot, T., Gossett, T. A., Gould, I. E., Palmstrom, A. F., Wolf, E. J., ... & McGehee, M. D. (2020). Improving low-bandgap tin–lead perovskite solar cells via contact engineering and gas quench processing. *ACS Energy Letters*, 5(4), 1215-1223.
12. Wang, C., Song, Z., Li, C., Zhao, D., & Yan, Y. (2019). Low-bandgap mixed tin–lead perovskites and their applications in all-perovskite tandem solar cells. *Advanced Functional Materials*, 29(47), 1808801.
13. Zhao, D., Yu, Y., Wang, C., Liao, W., Shrestha, N., Grice, C. R., ... & Yan, Y. (2017). Low-bandgap mixed tin–lead iodide perovskite absorbers with long carrier lifetimes for all-perovskite tandem solar cells. *Nature Energy*, 2(4), 1-7.
14. Euvrard, J., Yan, Y., & Mitzi, D. B. (2021). Electrical doping in halide perovskites. *Nature Reviews Materials*, 6(6), 531-549.
15. Kamat, P. V., & Kuno, M. (2021). Halide ion migration in perovskite nanocrystals and nanostructures. *Accounts of Chemical Research*, 54(3), 520-531.
16. Parveen, S., & Giri, P. K. (2022). Emerging doping strategies in two-dimensional hybrid perovskite semiconductors for cutting edge optoelectronics applications. *Nanoscale Advances*, 4(4), 995-1025.
17. Lee, H., Kang, S. B., Lee, S., Zhu, K., & Kim, D. H. (2023). Progress and outlook of Sn–Pb mixed perovskite solar cells. *Nano Convergence*, 10(1), 27.
18. Liu, Y., Chen, P. A., Qiu, X., Guo, J., Xia, J., Wei, H., ... & Hu, Y. (2022). Doping of Sn-based two-dimensional perovskite semiconductor for high-performance field-effect transistors and thermoelectric devices. *Iscience*, 25(4).
19. Jiang, Q., Chen, M., Li, J., Wang, M., Zeng, X., Besara, T., ... & Yu, Z. (2017). Electrochemical doping of halide perovskites with ion intercalation. *ACS nano*, 11(1), 1073-1079.



20. Qin, Z., Zhang, C., Chen, L., Wang, X., & Xiao, M. (2021). Charge carrier dynamics in Sn-doped two-dimensional lead halide perovskites studied by terahertz spectroscopy. *Frontiers in Energy Research*, *9*, 658270.
21. Juhi, J. P., Saski, M., Kochaniec, M. K., Wiczorek, W., Dominko, R., & Lewinski, J. (2025). Exploring Metal Halide Perovskites as Active Architectures in Energy Storage Systems. *Journal of Materials Chemistry A*.
22. Kumar, A., Suhail, A., Sagar Shukla, P., & Bag, M. (2024). Structural Stability of Mixed-Halide Perovskite Nanocrystals in Energy Storage: The Role of Iodine Expulsion. *ChemNanoMat*, *10*(11), e202400401.
23. Soltani, S., Ramesh, P., & Kim, J. (2025). Metal halide perovskites for energy applications: Recent advances, challenges, and future perspectives. *RSC Advances*, *15*(31), 21811–21837.